

Electron elastic scattering off $A@C_{60}$: The role of atomic polarization under confinement

V. K. Dolmatov,¹ M. Ya. Amusia,^{2,3} and L. V. Chernysheva³

¹*University of North Alabama, Florence, Alabama 35632, USA*

²*Racah Institute of Physics, Hebrew University, 91904 Jerusalem, Israel*

³*A. F. Ioffe Physical-Technical Institute, 194021 St. Petersburg, Russia*

(Dated: April 4, 2018)

The present paper explores possible features of electron elastic scattering off endohedral fullerenes $A@C_{60}$. It focuses on how dynamical polarization of the encapsulated atom A by an incident electron might alter scattering off $A@C_{60}$ compared to the static-atom- A case, as well as how the C_{60} confinement modifies the impact of atomic polarization on electron scattering compared to the free-atom case. The aim is to provide researchers with a “relative frame of reference” for understanding which part of the scattering processes could be due to electron scattering off the encapsulated atom and which due to scattering off the C_{60} cage. To meet the goal, the C_{60} cage is modeled by an attractive spherical potential of a certain inner radius, thickness, and depth which is a model used frequently in a great variety of fullerene studies to date. Then, the Dyson equation for the self-energy part of the Green’s function of an incident electron moving in the combined field of an encapsulated atom A and C_{60} is solved in order to account for the impact of dynamical polarization of the encaged atom upon $e + A@C_{60}$ scattering. The $Ba@C_{60}$ endohedral is chosen as the case study. The impact is found to be significant, and its utterly different role compared to that in $e + Ba$ scattering is unraveled.

PACS numbers: 31.15.ap, 31.15.V-, 34.80.Dp, 34.80.Bm

I. INTRODUCTION

Electron elastic scattering off quantum targets is an important fundamental phenomenon of nature. It has significance to both the basic and applied sciences and technologies. Yet, to date, the knowledge on the process of electron collision with such important quantum targets as endohedral fullerenes $A@C_{60}$ is far from complete. Endohedral fullerenes are nanostructure formations where an atom A is encapsulated inside the hollow interior of a C_{60} molecule. The authors are aware of only a handful of works on this subject. These are the theoretical studies of fast charged-particle ionization of $A@C_{60}$ [1–3] and low-energy electron scattering off $A@C_{60}$ [4–6] calculated in the framework of two different model approximations. Namely, in Refs. [4, 5] a static Hartree-Fock (HF) approximation was employed. There, both the atom A and C_{60} were considered as nonpolarizable targets and the C_{60} cage was modeled by an attractive spherical potential of a certain inner radius, thickness, and depth. In Ref. [6], the authors kept the encaged atom “frozen”, modeled the C_{60} cage by the potential similar to that used in Ref. [4, 5], but accounted for polarization of the C_{60} cage by incident electrons. The latter was evaluated in a simplified manner by adding a static polarization potential $-\alpha/r^4$ (α being the static polarizability of C_{60}) to the model C_{60} -potential. Note, a meager amount of research on $e + A@C_{60}$ collision is in contrast to the study of photon- $A@C_{60}$ collision, different aspect of which has been intensely scrutinized in a great variety of theoretical works to date (see, e.g., Refs. [7–14] and references therein), including experimental studies [15, 16] (and references therein). Such disbalance in favor of the number

and quality of studies of $A@C_{60}$ photoionization versus research on electron- $A@C_{60}$ collision is not accidental. Electronic collision with a multielectron target is a more complicated multifaceted process compared to photonic collision with the same target. Therefore, the comprehensive description of electron scattering by a multielectron target is too challenging for theorists even with regard to a free atom, not to mention $A@C_{60}$ targets.

The present study does not aim at solving the difficult problem of electron- $A@C_{60}$ scattering in its entirety. Instead, it focuses on the contribution of electron scattering only off the encapsulated atom A to the entire collision process. The significance of the present study is that it provides an important frame of reference for (future) understanding of which part of electron- $A@C_{60}$ scattering could be due to scattering off the encapsulated atom A (unraveled in the present work) and which is due to other “facets” of the entire $A@C_{60}$ system. Research results, thus, provide a relative rather than absolute knowledge. To meet the goal, the C_{60} cage is modeled, as in Refs. [4–6, 17], by a spherical potential of a certain inner radius, thickness, and depth. Polarization of the C_{60} cage by incident electrons will, thus, be ignored (being not the subject of the focused study). This is in contrast to accounting for polarization of the encapsulated atom in the present study. The neglect by polarizability of C_{60} by incident electrons should not be over-dramatized. The effect of polarizability is electron-energy-dependent and may either enhance or decrease scattering cross section, at certain electron energies. Therefore, when scattering off C_{60} is dramatically decreased, or where scattering of the encapsulated atom A is dramatically increased, a relative role of scattering off the atom A will (might) be

significant. Furthermore, $A@C_{60}$ has the hollow interior which is not totally occupied by the atom (i.e., not totally filled in with charge density). As such, it acts as a resonator relative to incident electronic waves. Therefore, at wave frequencies, matching resonance frequencies of the $A@C_{60}$ -resonator, there will be a significant incident-electron-density build-up in the hollow interior of $A@C_{60}$. Obviously, this build-up of electron density will be positioned near the encapsulated atom A . Therefore, the effect of atomic polarization on electron scattering might become comparable or even more important than the C_{60} polarization effect, at resonance frequencies. As such, the impact of atomic polarizability on $e+A@C_{60}$ scattering it cannot be dropped out of the consideration at all. It is, therefore, indisputably needed (and interesting, and does make sense) to study how polarization of the encapsulated atom can affect the scattering process even in the neglect by polarization of the fullerene cage by incident electrons. To account for atomic polarization under confinement, the authors employ the Dyson formalism for the self-energy part of the Green's function of a scattered electron [18, 19], adapt it to the case of the electron motion in a combined field of the encapsulated multielectron atom A and the model static C_{60} cage, solve the generalized Dyson equation, and, thus, calculate the electron elastic-scattering phase shifts and corresponding cross sections for the $e + A@C_{60}$ scattering reaction. The study is restricted to electron elastic scattering at low electron energies $\epsilon \lesssim 3$ eV where the most interesting effects occur.

Finally, the present study also has a significance which is independent of its direct applicability to electron- $A@C_{60}$ scattering. This is because it falls into a mainstream of intense modern studies where numerous aspects of the structure and spectra of atoms under various kinds of confinements (impenetrable spherical, spheroidal, dihedral, Debye-like potentials, etc.) are being attacked from many different angles by research teams world-wide (see, e.g., numerous review articles in Refs. [20–22]). Such studies are interesting from the view point of basic science. Results of the present study add new knowledge to the collection of atomic properties under confinement as well, particularly revealing the impact of atomic polarization under confinement on electron-atom scattering.

Atomic units are used throughout the paper unless specified otherwise.

II. THEORY

A. $e + A@C_{60}$ scattering in the framework of static C_{60}

1. Model static HF approximation

In the present work, the C_{60} cage is modeled by a spherical potential $U_c(r)$ defined as follows:

$$U_c(r) = \begin{cases} -U_0, & \text{if } r_0 \leq r \leq r_0 + \Delta \\ 0 & \text{otherwise.} \end{cases} \quad (1)$$

Here, r_0 , Δ , and U_0 are the inner radius, thickness, and depth of the potential well, respectively.

Next, the wavefunctions $\psi_{n\ell m_\ell m_s}(\mathbf{r}, \sigma) = r^{-1}P_{nl}(r)Y_{lm_\ell}(\theta, \phi)\chi_{m_s}(\sigma)$ and binding energies ϵ_{nl} of atomic electrons (n , ℓ , m_ℓ and m_s is the standard set of quantum numbers of an electron in a central field, σ is the electron spin variable) are the solutions of a system of the ‘‘endohedral’’ HF equations:

$$\left[-\frac{\Delta}{2} - \frac{Z}{r} + U_c(r) \right] \psi_i(\mathbf{x}) + \sum_{j=1}^Z \int \frac{\psi_j^*(\mathbf{x}')}{|\mathbf{x} - \mathbf{x}'|} \times [\psi_j(\mathbf{x}')\psi_i(\mathbf{x}) - \psi_i(\mathbf{x}')\psi_j(\mathbf{x})] d\mathbf{x}' = \epsilon_i \psi_i(\mathbf{x}). \quad (2)$$

Here, Z is the nuclear charge of the atom, $\mathbf{x} \equiv (\mathbf{r}, \sigma)$, and the integration over \mathbf{x} implies both the integration over \mathbf{r} and summation over σ . Eq. (2) differs from the ordinary HF equation for a free atom by the presence of the $U_c(r)$ potential in there. This equation is first solved in order to calculate the electronic ground-state wavefunctions of the encapsulated atom. Once the electronic ground-state wavefunctions are determined, they are plugged back into Eq. (2) in place of $\psi_j(\mathbf{x}')$ and $\psi_j(\mathbf{x})$ in order to calculate the electronic wavefunctions of scattering-states $\psi_i(\mathbf{x})$ and their radial parts $P_{\ell_i \ell_i}(r)$.

Corresponding electron elastic-scattering phase shifts $\delta_\ell(k)$ are then determined by referring to $P_{k\ell}(r)$ at large r :

$$P_{k\ell}(r) \rightarrow \sqrt{\frac{2}{\pi}} \sin \left(kr - \frac{\pi\ell}{2} + \delta_\ell(k) \right). \quad (3)$$

Here, k and k' are the wavenumbers of the incident and scattered electrons, respectively, and $P_{k\ell}(r)$ is normalized to $\delta(k - k')$. The total electron elastic-scattering cross section $\sigma_{el}(\epsilon)$ is then found in accordance with the standard formula for electron scattering by a central-potential field:

$$\sigma_{el}(k) = \frac{4\pi}{k^2} \sum_{\ell=0}^{\infty} (2\ell + 1) \sin^2 \delta_\ell(k). \quad (4)$$

This approach solves the problem of $e+A@C_{60}$ in a static approximation, i.e., without accounting for polarization of the $A@C_{60}$ system by incident electrons.

In the literature, some inconsistency is present in choosing the magnitudes of Δ , U_0 and r_0 of the model

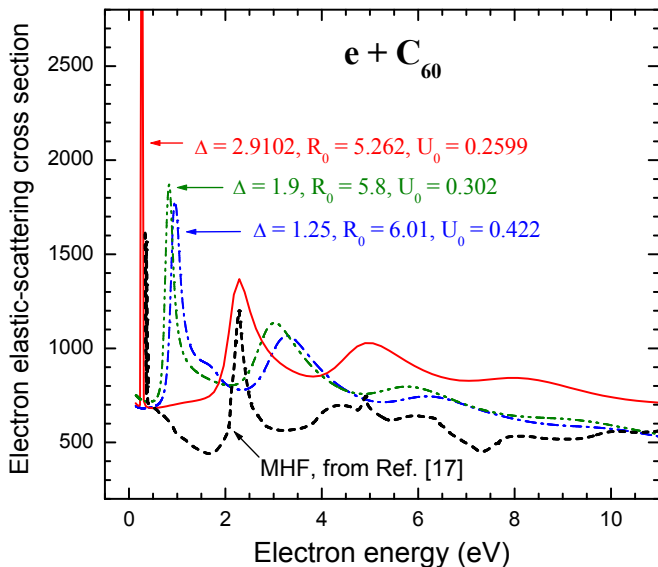


FIG. 1. (Color online) $e + C_{60}$ elastic-scattering cross section (in units of a_0^2 , a_0 being the first Bohr radius of the hydrogen atom) calculated both with the use of different values of the parameters r_0 , Δ , and U_0 of the spherical potential $U_c(r)$ (present work) and in the framework of *ab initio* MHF [17], as marked.

potential $U_c(r)$ for C_{60} : $r_0 = 5.8$, $\Delta = 1.9$, $U_0 = 0.302$ [8, 12] (and references therein), or $r_0 = 6.01$, $\Delta = 1.25$ and $U_0 = 0.422$ [2, 9], or $\Delta = 2.9102$, $r_0 = 5.262$, $U_0 = 0.2599$ [17]. In order to evaluate which of these sets of parameters is best suited for studying $e + A@C_{60}$ scattering, we performed the corresponding calculations of $e + C_{60}$ scattering. Calculated results are plotted in Fig. 1 against calculated data obtained in the framework of the sophisticated *ab initio* static-exchange molecular-Hartree-Fock (MHF) approximation [17].

One can see that it is the set of parameters proposed in Ref. [17] which leads [17] to the overall qualitative and semi-quantitative agreement between some of the most prominent features of $e + C_{60}$ elastic scattering predicted by the model spherical-potential approximation and *ab initio* MHF. Correspondingly, in the present work, as in Ref. [17], the $U_c(r)$ potential is defined by $\Delta = 2.9102$, $r_0 = 5.262$, and $U_0 = 0.2599$.

2. Multielectron approximation: a polarizable atom A

In order to account for the impact of polarization of an encapsulated atom A by incident electrons on $e + A@C_{60}$ elastic scattering, let us utilize the concept of the self-energy part of the Green's function of an incident electron [18, 19].

In the simplest second-order perturbation theory in the Coulomb interelectron interaction V between the incident and atomic electrons, the *irreducible* self-energy part of the Green's function $\Sigma(\epsilon)$ of the incident electron

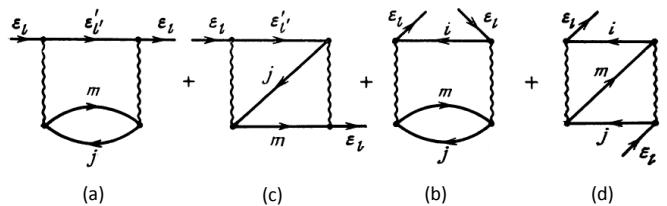


FIG. 2. The irreducible self-energy part $\Sigma(\epsilon)$ of the Green function of a scattering electron in the second-order perturbation theory in the Coulomb interaction, referred to as the SHIFT approximation (see text). Here, a line with a right arrow denotes an electron, whether a scattered electron (states $|\epsilon_\ell\rangle$ and $|\epsilon'_\ell\rangle$) or an atomic excited electron (a state $|m\rangle$), a line with a left arrow denotes a vacancy (hole) in the atom (states $|j\rangle$ and $|i\rangle$), a wavy line denotes the Coulomb interelectron interaction V .

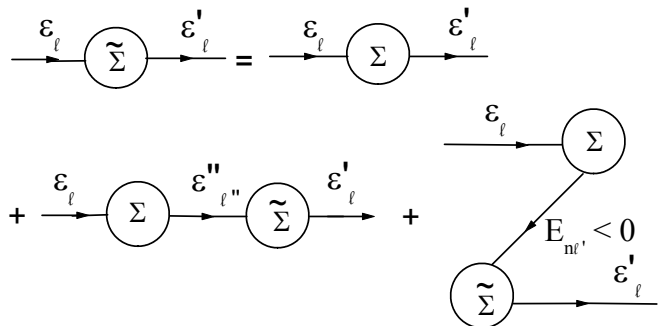


FIG. 3. The matrix element of the reducible self-energy part $\tilde{\Sigma}(\epsilon)$ of the Green's function of a scattering electron, where Σ is the irreducible self-energy part of the Green's function depicted in Fig. 2. This approximation is referred to as the SCAT approximation (see text). Note, when calculating $\langle \epsilon_\ell | \tilde{\Sigma} | \epsilon_\ell \rangle$ analytically, the summation over unoccupied discrete and integration over continuum excited states (marked as $\epsilon''_{\ell'}$) along with the summation over the occupied states in the atom marked as $E_{n\ell'}$ must be performed.

is depicted with the help of Feynman diagrams in Fig. 2.

The diagrams of Fig. 2 illustrate how a scattered electron “ ϵ_ℓ ” perturbs (read: polarizes) a j -subshell of the atom by causing $j \rightarrow m$ excitations from the subshell and then gets coupled with these excited states itself via both the Coulomb direct [diagrams (a) and (b)] and exchange [diagrams (c) and (d)] interactions. Numerical calculation of electron elastic-scattering phase shifts in the framework of this approximation is addressed by the computer code from Ref. [19] labeled as the “SHIFT” code. Correspondingly, the authors refer to this approximation as the “SHIFT” approximation everywhere in the present paper.

A fuller account of electron correlation (read: polarization) in $e + A@C_{60}$ elastic scattering is determined by the *reducible* $\tilde{\Sigma}(\epsilon)$ part of the self-energy part of the electron's Green function [19]. The matrix element of the latter are represented diagrammatically in Fig. 3.

The above diagrammatic equation for $\tilde{\Sigma}$ can be written in an operator form as follows:

$$\hat{\tilde{\Sigma}} = \hat{\Sigma} - \hat{\Sigma}\hat{G}^{(0)}\hat{\tilde{\Sigma}}. \quad (5)$$

Here, $\hat{\Sigma}$ is the operator of the irreducible self-energy part of the Green's function calculated in the framework of SHIFT (Fig. 2), $\hat{G}^{(0)} = (\hat{H}^{(0)} - \epsilon)^{-1}$ is the HF operator of the electron Green's function, and $\hat{H}^{(0)}$ is the HF Hamiltonian operator of the *electron* + $A@C_{60}$ system. Clearly, the equation for the matrix elements of $\tilde{\Sigma}$ accounts for an infinite series of diagrams by coupling the diagrams of Fig. 2 in various combinations. Numerical calculation of electron elastic-scattering phase shifts in the framework of this approximation is addressed by the computer code from Ref. [19] labeled as the ‘‘SCAT’’ code. Correspondingly, the authors refer to this approximation as the ‘‘SCAT’’ approximation everywhere in the present paper. SCAT works well for the case of electron scattering off free atoms [19]. This gives us confidence in that SCAT is a sufficient approximation for pinpointing the impact of correlation/polarization on $e + A@C_{60}$ scattering as well.

In the framework of SHIFT or SCAT, the electron elastic-scattering phase shifts ζ_ℓ are determined as follows [19]:

$$\zeta_\ell = \delta_\ell^{\text{HF}} + \Delta\delta_\ell. \quad (6)$$

Here, $\Delta\delta_\ell$ is the correlation/polarization correction term to the calculated HF phase shift δ_ℓ^{HF} :

$$\Delta\delta_\ell = \tan^{-1} \left(-\pi \langle \epsilon\ell | \tilde{\Sigma} | \epsilon\ell \rangle \right). \quad (7)$$

The mathematical expression for $\langle \epsilon\ell | \tilde{\Sigma} | \epsilon\ell \rangle$ is cumbersome. The interested reader is referred to [19] for details. The matrix element $\langle \epsilon\ell | \tilde{\Sigma} | \epsilon\ell \rangle$ becomes complex for electron energies exceeding the ionization potential of the atom-target, and so does the correlation term $\Delta\delta_\ell$ and, thus, the phase shift ζ_ℓ as well. Correspondingly,

$$\zeta_\ell = \delta_\ell + i\mu_\ell, \quad (8)$$

where

$$\delta_\ell = \delta_\ell^{\text{HF}} + \text{Re}\Delta\delta_\ell, \quad \mu_\ell = \text{Im}\Delta\delta_\ell. \quad (9)$$

The total electron elastic-scattering cross section σ_{el} is then given by the expression

$$\sigma_{\text{el}} = \sum_{\ell=0}^{\infty} \sigma_\ell, \quad (10)$$

where σ_ℓ is the electron elastic-scattering partial cross section:

$$\sigma_\ell = \frac{2\pi}{k^2} (2\ell + 1) \frac{\cosh 2\mu_\ell - \cos 2\delta_\ell}{e^{2\mu_\ell}}. \quad (11)$$

III. RESULTS AND DISCUSSION: $e + \text{Ba}@C_{60}$ SCATTERING

3. Preliminary notes

In the aims of the present paper, the authors focus on electron scattering off $\text{Ba}@C_{60}$, as the case study. This is because the Ba atom is a highly polarizable atom. It is expected to retain its high polarizability under the C_{60} confinement as well. This provides one with a better opportunity to learn how atomic polarization can alter electron scattering off $A@C_{60}$ compared to scattering off the static target.

Furthermore, the study focuses on the electron energy region of up to $\epsilon \approx 3$ eV. First, at such energies, the electron wavelength $\lambda > 6$ Å exceeds greatly the bond length $D \approx 1.44$ Å between the carbon atoms in C_{60} . Correspondingly, the incoming electrons will ‘‘see’’ the C_{60} cage as a homogeneous rather than ‘‘granular’’ cage. This makes it appropriate to model the C_{60} cage by a non-granular, i.e., ‘‘smooth’’ potential. Moreover, as was shown in Refs. [23, 24], a low-energy electron motion in the field of C_{60} is insensitive to details of the ‘‘smooth’’ potential, i.e., to whether the potential is the potential with round borders and unparallel walls or simply a square-well potential, as long as $\lambda \gg D$. This additionally justifies the use of the square-well potential, Eq. (1), in the present study. Second, correlation/polarization effects, which are of the primary concern of this paper, are expected, as usually, to be most strong primarily at low-energy electron collisions with multielectron targets. Third, at these low energies, earlier, there were predicted spectacular confinement-induced resonances in $e + A@C_{60}$ scattering [4, 5], similar to those predicted in $e + C_{60}$ scattering [5, 17, 25]. The presence of the confining C_{60} cage in this case, as well as in the case of scattering off empty C_{60} , results in the emergence of positive quasi-discrete states in the field of $A@C_{60}$ or C_{60} . When quasi-discrete states are present, then, in accordance with the known fact, ‘‘... resonance scattering occurs because a positive level with $\ell \neq 0$, though not a true discrete level, is quasi-discrete: owing to the presence of the centrifugal potential barrier, the probability that a particle of low energy will escape from this state to infinity is small, so that the lifetime of the state is long’’ [26].

It is interesting to explore how the predicted resonances in $e + A@C_{60}$ scattering can be altered by the effects of polarization of the encapsulated atom A by incident electrons.

Next, the calculations of electron scattering off $\text{Ba}@C_{60}$ and free Ba, performed in the present work in the framework of both SHIFT and SCAT, accounted for the monopole, dipole, quadrupole, and octupole perturbations of the valence $6s^2$ and $5p^6$ subshells of free and encaged Ba by incident electrons. Finally, in view of low values of the electron energies, only the s -, p -, d -, f -, and g -partial electronic waves have been accounted for in the calculations. The contribution of other partial electronic

waves is negligible, at given energies.

4. Results and discussion

Corresponding calculated HF, SHIFT, and SCAT data for the real parts of phase shifts $\delta_\ell(\epsilon)$, partial $\sigma_\ell(\epsilon)$ and total $\sigma_{\text{el}}(\epsilon)$ cross sections for electron elastic scattering off Ba@C₆₀ are displayed in Fig. 4 (the imaginary parts μ_ℓ of the phase shifts, when present, are small at the chosen energies and present little interest for discussion).

As an important finding, one learns from Fig. 4 that the C₆₀ confinement does not at all “extinguish” the possibility for the encapsulated Ba atom to be strongly polarized by incident electrons. On the contrary, the polarization impact is found to affect dramatically both the electron scattering phase shifts and partial σ_ℓ as well as total σ_{el} cross sections. All this is obvious from the comparison of calculated results obtained in the framework of HF, on the one hand, and SHIFT and SCAT, on the other hand, approximations. As another important result, one finds that accounting for only the second-order (with respect to the Coulomb interaction) correlation effects, as in SHIFT, is important but far insufficient for the calculation of low-energy electron scattering off Ba@C₆₀. Indeed, the correlation impact beyond the second-order approximation, i.e., accounted for in the SCAT approximation, is utterly significant – the lower the energy, the stronger the impact.

For the next, it is both interesting and necessary to bring to the attention of the reader that the *empty* static C₆₀ cage can only support the *s*-, *p*-, and *d*-bound states [5, 17]. In contrast, the “stuffed” C₆₀, i.e., Ba@C₆₀, was found to lose a *s*-bound state, but acquire, instead, a *f*-bound state, in the static HF approximation [5]. Now, it follows from the present study that by “unfreezing” the encapsulated Ba atom, i.e., by making it polarizable, the lost *s*-bound state is returned to the Ba@C₆₀ system, and the latter keeps the former *p*-, *d*- and *f*-bound states. Moreover, the Ba@C₆₀ system is found to start supporting a second *p*-bound state as well. All this becomes clear by noting the calculated SCAT values of the *s*-, *p*-, *d*-, and *f*-phase shifts at $\epsilon \rightarrow 0$: $\delta_s^{\text{SCAT}} \rightarrow 7\pi$, $\delta_p^{\text{SCAT}} \rightarrow 6\pi$, $\delta_d^{\text{SCAT}} \rightarrow 3\pi$, and $\delta_f^{\text{SCAT}} \rightarrow \pi$. The zero-energy values of these phase shifts satisfy the generalized version of Levinson theorem for scattering in a potential field [26] which (the generalized theorem) could be derived by the direct numerical calculation and written as follows:

$$\delta_\ell(\epsilon)|_{\epsilon \rightarrow 0} \rightarrow (N_{n_\ell} + q_\ell)\pi. \quad (12)$$

Here, N_{n_ℓ} is the number of closed subshells with given ℓ in the ground-state configuration of an atom, whereas q_ℓ is the number of additional *empty* bound states with the same ℓ in the field of A@C₆₀. Given that, for the ground-state of the encapsulated Ba atom, $N_{n_s} = 6$, $N_{n_p} = 4$, $N_{n_d} = 2$, and $N_{n_f} = 0$, one finds that, in accordance with the SCAT values of the phase shifts,

$q_{n_s} = 1$, $q_{n_p} = 2$, $q_{n_d} = 1$, and $q_{n_f} = 1$. This translates into one *s*-, two *p*-, one *d*-, and one *f*-bound states supported (one at a time) by Ba@C₆₀. Note that calculated SHIFT phase shifts, in contrast to SCAT data, point to the existence of neither *s*- nor second *p*-bound state in the field of Ba@C₆₀. This discrepancy between the calculated SHIFT and SCAT data speaks, in general, to the importance of a fuller account of electron correlation in the calculation of *e*+A@C₆₀ scattering.

The discovered in the framework of SCAT emergence of a *s*-bound state and a second *p*-bound state in the field of Ba@C₆₀ has profound consequences for both the corresponding partial and total electron-scattering cross sections. Namely, because the phase shift δ_s^{SCAT} , on the way to its value of 7π at $\epsilon = 0$, passes through the value of modulo $\pi/2$ (at $\epsilon \approx 0.23$ eV), σ_s^{SCAT} becomes large, at lower energies, in contrast to the predictions obtained with the help of inferior HF and SHIFT. Similarly, the increase of δ_p^{SCAT} to 6π at $\epsilon = 0$ results in large σ_p^{SCAT} as well, at low energies, again, in contrast to the predictions by HF and SHIFT.

Talking about the *d*- and *g*-partial cross sections, one can see that each of them is dominated by the strong resonance. Its emergence clearly follows from the behavior of the *d*- and *g*-phase shifts. Indeed, the phase shifts first tend to increase towards modulo π with decreasing energy, but, because the field turns out to be not strong enough, before that value is reached, they sharply decrease, passing through the value of modulo $\pi/2$. This is a typical behavior of phase shifts upon electron scattering on quasibound states [27]. Next, note how the resonances in the *d*- and *g*-partial cross sections become higher, narrower, and shift towards lower energy as more correlation is accounted for in the calculation (compare calculated HF versus SHIFT versus SCAT results). We thus find that the inclusion of more correlation into the calculation of *e* + Ba@C₆₀ scattering increases the strength of the field of the Ba@C₆₀-scatterer, since the above noted changes in the resonances are typical for electron scattering in a field of increasing strength [27].

Next, note that no *f*-resonance emerges in *e* + Ba@C₆₀ scattering calculated in either of the three approximations utilized in this paper. This is in contrast to electron elastic-scattering off empty static C₆₀. There, the sharp *f*-resonance was predicted to emerge at low energies [5, 17, 25] (this is the extremely narrow resonance near zero plotted in Fig. 1). The reason for the absence of the *f*-resonance in *e* + Ba@C₆₀ scattering is interesting. It is directly associated with that a noticeable part of the valence electronic charge-density of encapsulated Ba is drawn into the C₆₀ shell [5]. Therefore, the field inside the “stuffed” C₆₀ becomes more attractive than in empty C₆₀. It turns the *f*-state into a bound state, thereby eliminating the emergence of a *f*-resonance in *e* + Ba@C₆₀ scattering. Now, as it has been shown in the paragraph above, the inclusion of correlation into the calculation of *e* + Ba@C₆₀ scattering increases the field of Ba@C₆₀. Therefore, the *f*-state remains bound. This is why the

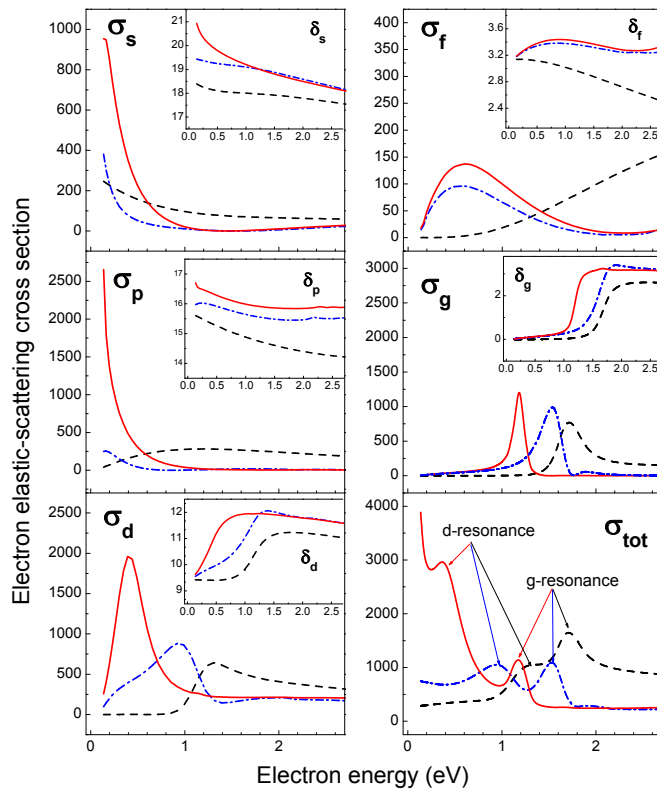


FIG. 4. (Color online) Main panels: Calculated partial $\sigma_{\ell}(\epsilon)$ and total $\sigma_{\text{el}}(\epsilon)$ cross sections (in units of a_0^2) for electron elastic scattering off $\text{Ba}@C_{60}$, obtained in the frameworks of the model static HF (dashed line), multielectron SHIFT (dash-dotted line) and SCAT (solid line) approximations. Insets: Real parts $\delta_{\ell}(\epsilon)$ of the phase shifts $\zeta_{\ell}(\epsilon)$ (in units of radian) calculated in HF (dashed line), multielectron SHIFT (dash-dotted line) and SCAT (solid line) approximations.

f -resonance does not take place in $e + \text{Ba}@C_{60}$ scattering even if polarization of the encapsulated Ba atom by incident electrons is accounted for in the calculation. Our general prediction is that there will be no f -resonances on quasibound states in electron scattering off any $A@C_{60}$ system in case where there is a noticeable transfer of electronic charge-density from the encapsulated atom to the C_{60} shell.

Furthermore, it is interesting to compare how much differently polarization of the Ba atom by incident electrons affects electron elastic scattering off free Ba versus $\text{Ba}@C_{60}$. The corresponding calculated HF and SCAT total electron elastic-scattering cross sections are depicted in Fig. 5.

The calculated data reveal a spectacular difference between the role of polarization in electron scattering off Ba and $\text{Ba}@C_{60}$. Namely, it appears that the effects of polarization in $e + \text{Ba}@C_{60}$ scattering act oppositely to the effects in $e + \text{Ba}$ scattering. Thus, whereas $\sigma_{\text{el}}^{\text{SCAT}}(e + \text{Ba}) \ll \sigma_{\text{el}}^{\text{HF}}(e + \text{Ba})$ at $\epsilon \lesssim 1$ eV, the situation is exact opposite for $e + \text{Ba}@C_{60}$ scattering in about the same energy region: $\sigma_{\text{el}}^{\text{SCAT}}(e + \text{Ba}@C_{60}) \gg \sigma_{\text{el}}^{\text{HF}}(e + \text{Ba}@C_{60})$. Alternatively, whereas $\sigma_{\text{el}}^{\text{SCAT}}(e + \text{Ba}) \gg \sigma_{\text{el}}^{\text{HF}}(e + \text{Ba})$ at $\epsilon \gtrsim 1.4$ eV, one observes that $\sigma_{\text{el}}^{\text{SCAT}}(e + \text{Ba}@C_{60}) \ll \sigma_{\text{el}}^{\text{HF}}(e + \text{Ba}@C_{60})$ in there. It is, thus, found in the present study that the effects of atomic polarization in electron

scattering off the free and encapsulated inside C_{60} atoms may follow opposite routes. This is an interesting observation.

Lastly, note that there are energy regions, specifically, $0.8 \lesssim \epsilon \lesssim 1.1$ eV and $\epsilon \gtrsim 1.2$ eV, where $\sigma_{\text{el}}^{\text{SCAT}}(e + \text{Ba}@C_{60}) \ll \sigma_{\text{el}}^{\text{SCAT}}(e + \text{Ba})$. This means that the gas-medium of big-sized $A@C_{60}$ s can be more transparent to incident electrons than the gas-medium of smaller-sized isolated atoms A themselves. This counter-intuitive effect was earlier unveiled in Ref. [4] in the framework of the static HF approximation, but appears to retain its place even if the encapsulated atom is polarizable, as is shown in the present paper.

IV. CONCLUSION

The present work has provided a deeper insight into possible features of low-energy electron elastic scattering off $A@C_{60}$ fullerenes. This has been achieved by studying the dependence of $e + \text{Ba}@C_{60}$ elastic scattering with account for polarization of encapsulated Ba by incident electrons. It has been demonstrated that the polarization effect results in dramatic differences between electron scattering off $\text{Ba}@C_{60}$ evaluated with and without inclusion of polarization into the calculation. It has

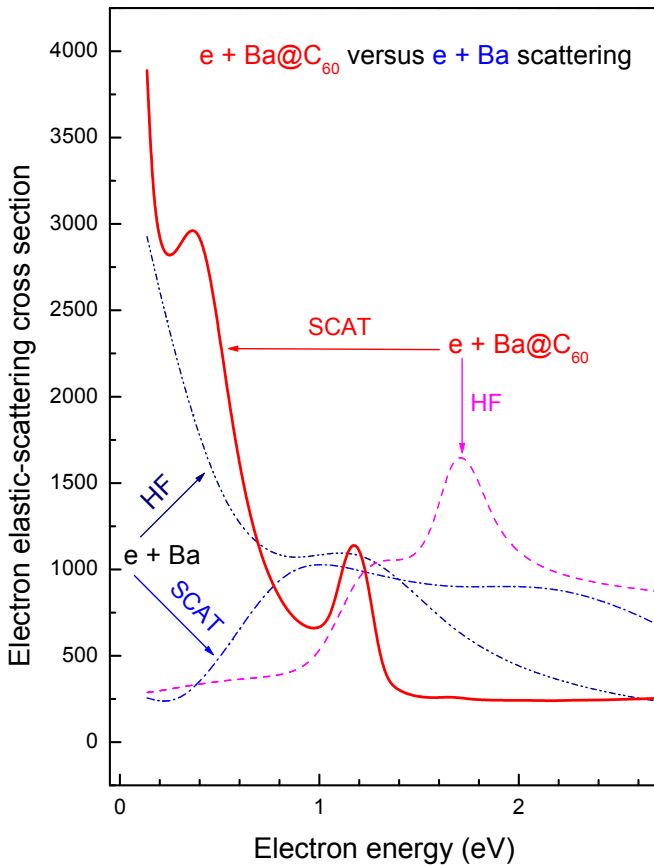


FIG. 5. (Color online) Calculated total electron elastic-scattering cross sections $\sigma_{el}(\epsilon)$ (in units of a_0^2) for electron scattering off $Ba@C_{60}$, obtained in the frameworks of the model static HF (dashed line) and multielectron SCAT (solid line) approximations, as well as off free Ba (HF, dash-dot-dot; SCAT, dash-dot), as marked.

been found that a fuller account for correlation effects in $e + A@C_{60}$ scattering is utterly important. Furthermore, it has been unraveled in the present study that the impact of polarization on electron scattering off $A@C_{60}$ may be both qualitatively and quantitatively different than that in the case of electron scattering by the free atom A . For instance, it has been demonstrated that where polarization significantly enhances the $e + Ba@C_{60}$ scattering cross section, it significantly diminishes the $e + Ba$ scattering cross section and vice versa. This leads to the possibility for electron scattering off $A@C_{60}$ to become significantly weaker than in the case of electron scattering by the isolated atom A , in certain energy regions. This counter-intuitive effect has been found to be stronger and occur in a broader energy region than when polarization is ignored.

Lastly, the present study provides researchers with background information which is useful for future studies of electron scattering by $A@C_{60}$, particularly aimed at elucidating of a possible significance of a simultaneous polarization of both the C_{60} cage and engaged atom by incident electrons. This will make the $A@C_{60}$ more attractive, so that predicted in the present study features of $e + A@C_{60}$ may appear at different energies, or disappear at all, some actual bound states may be converted to resonances, etc. Such effects, however, are subject to an independent study.

V. ACKNOWLEDGEMENTS

V.K.D. acknowledges the support by NSF Grant No. PHY-1305085.

REFERENCES

- [1] A. S. Baltenkov, V. K. Dolmatov, S. T. Manson, and A. Z. Msezane, Fast charged-particle impact ionization of endohedral atoms, *Phys. Rev. A* **79**, 043201 (2009). DOI: 10.1103/PhysRevA.79.043201
- [2] M. Ya. Amusia, L. V. Chernysheva, and V. K. Dolmatov, Confinement and correlation effects in the $Xe@C_{60}$ generalized oscillator strengths, *Phys. Rev. A* **84**, 063201 (2011). DOI: 10.1103/PhysRevA.84.063201
- [3] R. Cabrera-Trujillo and S. A. Cruz, Confinement approach to pressure effects on the dipole and the generalized oscillator strength of atomic hydrogen, *Phys. Rev. A* **87**, 012502 (2013). DOI: 10.1103/PhysRevA.87.012502
- [4] V. K. Dolmatov, M. B. Cooper, and M. E. Hunter, Electron elastic scattering off endohedral fullerenes $A@C_{60}$: The initial insight, *J. Phys. B* **47**, 115002 (2014). DOI: 10.1088/0953-4075/47/11/115002
- [5] V. K. Dolmatov, C. Bayens, M. B. Cooper, and M. E. Hunter, Electron elastic scattering and low-frequency bremsstrahlung on $A@C_{60}$: A model static-exchange approximation, *Phys. Rev. A* **91**, 062703 (2015). DOI: 10.1103/PhysRevA.91.062703
- [6] M. Ya. Amusia and L. V. Chernysheva, On the behavior of scattering phases in collisions of electrons with multi-atomic objects, *JETP Lett.* **100**, 503 (2015). DOI: 10.1134/S0021364014210024
- [7] A. S. Baltenkov, Resonances in photoionization cross sections of inner subshells of atoms inside the fullerene cage, *J. Phys. B* **32**, 2745 (1999). DOI: 10.1088/0953-4075/32/11/320
- [8] J.-P. Connerade, V. K. Dolmatov, and S. T. Manson, A unique situation for an endohedral metallofullerene, *J. Phys. B* **32**, L395 (1999). DOI: 10.1088/0953-4075/32/14/108
- [9] T. W. Gorczyca, M. F. Hasoglu, and S. T. Manson, Photoionization of endohedral atoms using R-matrix methods: Application to $Xe@C_{60}$, *Phys. Rev. A* **86**, 033204 (2012). DOI: 10.1103/PhysRevA.86.033204

- [10] M. Ya. Amusia and L. V. Chernysheva, Comment on “Photoionization of endohedral atoms using R-matrix methods: application to Xe@C₆₀”, *Phys. Rev. A* **89**, 057401 (2014). DOI: 10.1103/PhysRevA.89.057401
- [11] M. Ya. Amusia, L. V. Chernysheva, and E. G. Drukarev, Explanation of the recent results on photoionization of endohedral atoms, *JETP Lett.* **100**, 543 (2015). DOI: 10.1134/S0021364014210024
- [12] Bowen Li, Gerry O’Sullivan, and Chenzhong Dong, Relativistic R-matrix calculation photoionization cross section of Xe and Xe@C₆₀, *J. Phys. B* **46**, 155203 (2013). DOI: 10.1088/0953-4075/46/15/155203
- [13] P. C. Deshmukh, A. Mandal, S. Saha, A. S. Kheifets, V. K. Dolmatov, and S. T. Manson, Attosecond time delay in the photoionization of endohedral atoms A@C₆₀: A probe of confinement resonances, *Phys. Rev. A* **89**, 053424 (2014). DOI: 10.1103/PhysRevA.89.053424
- [14] Mohammad H. Javani, Jacob B. Wise, Ruma De, Mohamed E. Madjet, Steven T. Manson, and Himadri S. Chakraborty, Resonant Auger-intersite-Coulombic hybridized decay in the photoionization of endohedral fullerenes, *Phys. Rev. A* **89**, 063420 (2014). DOI: 10.1103/PhysRevA.89.063420
- [15] A. L. D. Kilcoyne, A. Aguilar, A. Müller, S. Schippers, C. Cisneros, G. AlnaWashi, N. B. Aryal, K. K. Baral, D. A. Esteves, C. M. Thomas, and R. A. Phaneuf, Confinement Resonances in Photoionization of Xe@C₆₀⁺, *Phys. Rev. Lett.* **105**, 213001 (2010). DOI: 10.1103/PhysRevLett.105.213001
- [16] R. A. Phaneuf, A. L. D. Kilcoyne, N. B. Aryal, K. K. Baral, D. A. Esteves-Macaluso, C. M. Thomas, J. Hellhund, R. Lomsadze, T. W. Gorczyca, C. P. Ballance, S. T. Manson, M. F. Hasoglu, S. Schippers, and A. Müller, Probing confinement resonances by photoionizing Xe inside a C₆₀⁺ molecular cage, *Phys. Rev. A* **88**, 053402 (2013). DOI: 10.1103/PhysRevA.88.053402
- [17] C. Winstead and V. McKoy, Elastic electron scattering by fullerene, C₆₀, *Phys. Rev. A* **73**, 012711 (2006). DOI: 10.1103/PhysRevA.73.012711
- [18] A. A. Abrikosov, L. P. Gorkov, and I. E. Dzyaloshinski, *Methods of Quantum Field Theory in Statistical Physics*, edited by R. A. Silverman (Prentice-Hall, Englewood Cliffs, NJ, 1963).
- [19] M. Ya. Amusia and L. V. Chernysheva, *Computation of Atomic Processes: A Handbook for the ATOM Programs* (IOP, Bristol, 1997).
- [20] *Theory of Confined Quantum Systems: Part 1*, edited by J. R. Sabin, E. Brändas, and C. A. Cruz, *Advances in Quantum Chemistry*, Vol. 57 (Academic Press, New York, 2009).
- [21] *Theory of Confined Quantum Systems: Part 2*, edited by J. R. Sabin, E. Brändas, and C. A. Cruz, *Advances in Quantum Chemistry*, Vol. 58 (Academic Press, New York, 2009).
- [22] *Electronic Structure of Quantum Confined Atoms and Molecules*, edited by K. D. Sen (Springer International Publishing, Switzerland, 2014).
- [23] V. K. Dolmatov, J. L. King, and J. C. Oglesby, Diffuse versus square-well confining potentials in modelling A@C₆₀ atoms, *J. Phys. B* **45**, 105102 (2012). DOI: 10.1088/0953-4075/45/10/105102; [Corrigendum in: *J. Phys. B* **48**, 069501 (2015). DOI: 10.1088/0953-4075/48/6/069501]
- [24] A. S. Baltenkov, S. T. Manson, and A. Z. Msezane, Jellium model potentials for the C₆₀ molecule and the photoionization of endohedral atoms, A@C₆₀, *J. Phys. B* **48**, 185103 (2015). DOI: 10.1088/0953-4075/48/18/185103
- [25] M. Ya. Amusia, A. S. Baltenkov, and B. G. Krakov, Photodetachment of negative C₆₀⁻ ions, *Phys. Lett. A* **243**, 99 (1998). DOI: 10.1016/S0375-9601(98)00158-3
- [26] L. D. Landau and E. M. Lifshitz, *Quantum Mechanics: Nonrelativistic theory* (Butterworth-Heinemann, Boston, 2002).
- [27] R. G. Newton, *Scattering Theory of Wave and Particles* (McGraw-Hill, New York, 1969).